Mandelpinski Spokes in the Parameter Planes of Rational Maps *

Robert L. Devaney†
Department of Mathematics
Boston University
111 Cummington Mall
Boston, MA 02215 USA

September 1, 2015

*2000 MSC number: Primary 37F10; Secondary 37F45

†Robert L. Devaney was partially supported by Simons Foundation Grant #208780

Abstract

In this paper we describe a new structure that arises in the parameter plane of the family of maps $z^n + \lambda/z^d$ where $n \geq 2$ is even but $d \geq 3$ is odd. We call these structures Mandelbrot-Sierpiński spokes (or, for short, "Mandelpinski spokes"). It is known that there are infinitely many baby Mandelbrot sets in these parameter planes that are part of what is called the Mandelpinski maze for these maps. We show here that there are infinitely many "spokes" emanating from each of these Mandelbrot sets. Each spoke consists of infinitely many alternating Mandelbrot sets and Sierpiński holes that lie along a certain arc that tends away from the given Mandelbrot set in a certain direction.

In this paper we will concentrate on the family of maps $F_\lambda(z) = z^2 + \lambda/z^3$, though everything we discuss goes over to the more general case of $z^n + \lambda/z^d$ where $n \geq 2$ is even $d \geq 3$ is odd. It is known [4] that there is a very elaborate structure called a Mandelpinski maze that branches away from the negative real axis in the parameter planes for these maps. Roughly speaking, this maze consists of infinitely many baby Mandelbrot sets and Sierpiński holes that alternate along each edge of a specific planar graph that has infinitely many vertices. A Sierpiński hole is a disk in which all parameters correspond to maps whose Julia sets are Sierpiński curves, i.e., they are homeomorphic to the well known Sierpiński carpet.

In this paper we will look in detail at a neighborhood of each of these Mandelbrot sets in the maze. We shall show that there are infinitely many "spokes" emanating from this set. Along these spokes there are infinitely many alternating copies of Mandelbrot sets and Sierpiński holes. Roughly speaking, the spokes along which these sets lie are the analogues of the external rays of angle $j/2^k$ in the parameter plane for the usual Mandelbrot set, though, of course, in this case, these rays are not in the region where the critical values lie in the basin of ∞.

In Figures 1 and 2, we display the parameter plane for $z^2 + \lambda/z^3$, i.e., the λ-plane. Along the negative real axis, there are infinitely many disks: these are the Sierpiński holes. Between any two Sierpiński holes, there is then a (very small) Mandelbrot set, as shown in the first magnification in this figure. Each of the four spokes displayed in this magnification pass through infinitely many more Mandelbrot sets and Sierpiński holes. The next two magnifications in Figure 2 show more of the spokes emanating from this Mandelbrot set. The Sierpiński holes are again visible, but the intermediate Mandelbrot sets are too small to be seen at this level.

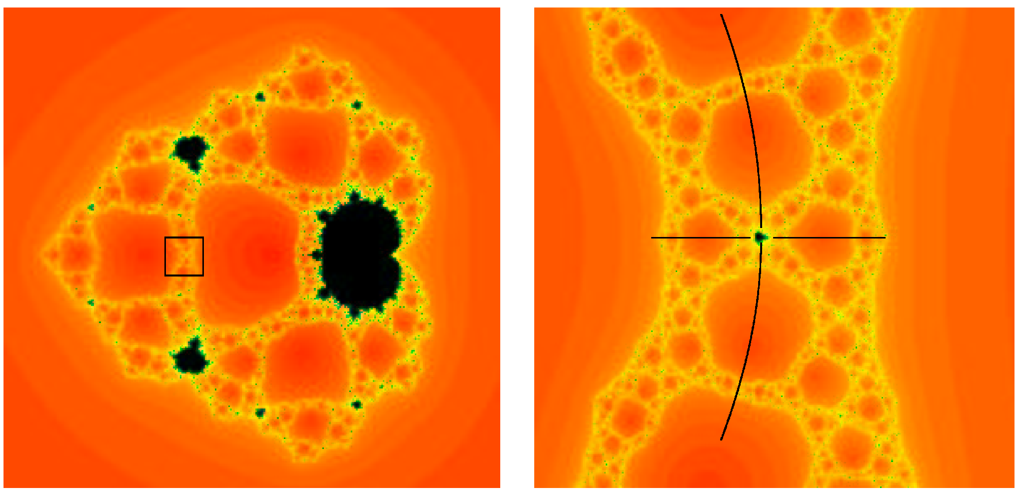

Figure 1: The parameter plane for $z^2 + \lambda/z^3$. The magnification shows a small Mandelbrot set with four spokes $(0, 1/4, 1/2, 3/4)$ emanating. Figure 2 shows further magnifications around this Mandelbrot set.

As mentioned above, all of the results below hold for the more general families given by $z^n + \lambda/z^d$ where $n > 1$ is even and $d > 1$ is odd. The associated structures are then symmetrically located around the origin via an $(n-1)$-fold symmetry. See [1]. This may be seen in Figure 3 where the parameter plane for $z^4 + \lambda/z^3$ is displayed.

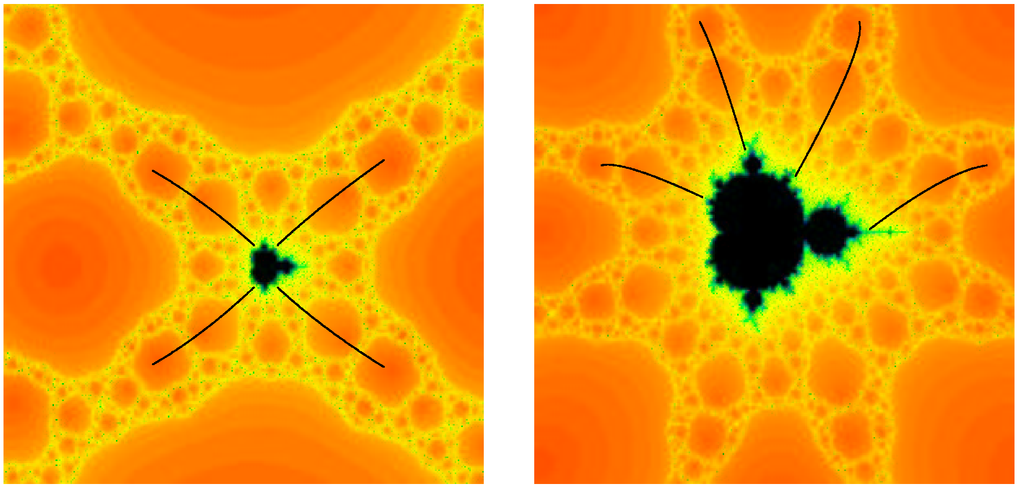

Figure 2: Two further magnifications of the parameter plane. In the first figure, the spokes with angle $j/8$ where $j = 1, 3, 5$, and 7 are displayed, and, in the second, those with angle $j/16$ where $j = 1, 3, 5$, and 7 are displayed. Again, the intermediate Mandelbrot sets are too small to be seen.

1 Preliminaries

This paper describes what we call the Mandelpinski spokes that live in the parameter plane of the family of rational maps given by

$$F_\lambda(z) = z^n + \frac{\lambda}{z^d}$$

where $n \geq 2$ is even and $d \geq 3$ is odd. However, for simplicity, we shall concentrate only on the case

$$F_\lambda(z) = z^2 + \frac{\lambda}{z^3}.$$

The extensions from this case to the more general case are straightforward; see [4] for more details.

When $|z|$ is large, we have that $|F_\lambda(z)| > |z|$ and so the point at ∞ is an attracting fixed point in the Riemann sphere. We denote the immediate

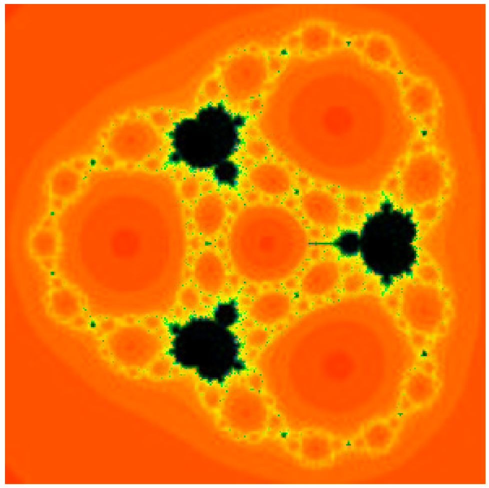

Figure 3: The parameter plane for the family $z^4 + \lambda/z^3$.

basin of attraction of ∞ by B_λ. There is also a pole at the origin for each of these maps, and so there is a neighborhood of the origin that is mapped into B_λ. If the preimage of B_λ surrounding the origin is disjoint from B_λ, we call this region the trap door and denote it by T_λ.

The Julia set of F_λ, $J(F_\lambda)$, has several equivalent definitions. $J(F_\lambda)$ is the set of all points at which the family of iterates of F_λ fails to be a normal family in the sense of Montel. Equivalently, $J(F_\lambda)$ is the closure of the set of repelling periodic points of F_λ, and it is also the boundary of the set of all points whose orbits tend to ∞ under iteration of F_λ, not just those in the boundary of B_λ. See [11].

There are five critical points for the map F_λ that are given by $(3\lambda/2)^{1/5}$. We denote the critical point that lies in $\mathbb{R}^-$ when $\lambda \in \mathbb{R}^-$ by $c_0 = c_0^\lambda$ (and then c_0^λ varies analytically with λ). We denote the other critical points by $c_j = c_j^\lambda$ for $-2 \leq j \leq 2$ where the c_j are now arranged in the clockwise order as j increases. As λ moves half way around the origin from $\mathbb{R}^-$, c_0 rotates exactly one-tenth of a turn in the corresponding direction. Thus, when $\operatorname{Arg}\lambda$ decreases from π to 0, c_2 lies in $\mathbb{R}^+$ and when $\operatorname{Arg}\lambda$ increases from π to 2π, c_{-2} now lies in $\mathbb{R}^+$. The critical values of F_λ are then given by $v^\lambda = \kappa\lambda^{2/5}$ where κ is the constant given by $5/(2^{2/5}3^{3/5})$. One computes easily that $\kappa \approx 1.96$. We denote by v_j^λ the critical value that is the image of c_j^λ.

There are also five prepoles for F_λ given by $(-\lambda)^{1/5}$. We denote the prepole that lies in $\mathbb{R}^+$ when $\lambda \in \mathbb{R}^-$ by $p_2 = p_2^\lambda$. The other prepoles are denoted by $p_j = p_j^\lambda$ where again $-2 \leq j \leq 2$ and the p_j are arranged in the clockwise order as j increases. Note that, when $\lambda \in \mathbb{R}^-$, the critical point c_0 lies between the two rays starting at the origin and passing through p_0 and p_{-1}.

The straight ray extending from the origin to ∞ and passing through the critical point c_j^λ is called a *critical point ray.* This ray is mapped two-to-one onto the portion of the straight ray from the origin to ∞ that starts at the critical value v_j^λ and extends to ∞. A similar straight line extending from 0 to ∞ and passing through a prepole p_j^λ is a *prepole ray*, and this ray is mapped one-to-one onto the entire straight line passing through both the origin and the point $(-\lambda)^{2/5}$. Note that all five of these points are different, so there are five different images of the prepole rays.

Let ω be a fifth root of unity. Then we have $F_\lambda(\omega z) = \omega^2 F_\lambda(z)$, and so it follows that the dynamical plane is symmetric under the rotation $z \mapsto \omega z$. In particular, all of the critical orbits have "similar" fates. If one critical orbit tends to ∞, then all must do so. If one critical orbit tends to an attracting cycle of some period, then all other critical orbits also tend to an attracting cycle, though these cycles may be different and also may have different periods. Nonetheless, the points on these attracting cycles are all symmetrically located with respect to the rotation by ω. As a consequence, each of B_λ, T_λ, and $J(F_\lambda)$ are symmetric under rotations by ω.

There is an Escape Trichotomy [7] for this family of maps. One scenario in this trichotomy occurs when one and hence, by symmetry, all of the critical values lie in B_λ. In this case it is known that $J(F_\lambda)$ is a Cantor set. The corresponding set of λ-values in the parameter plane is called the Cantor set locus. The second scenario is that the critical values all lie in T_λ (which we assume is disjoint from B_λ). In this case the Julia set is a Cantor set of simple closed curves surrounding the origin. This can only happen when $n, d \geq 2$ but not both equal to 2 [10]. We call the region $\mathcal{E}^1$ in parameter plane where this occurs the "McMullen domain"; it is known that $\mathcal{E}^1$ is an open disk surrounding the origin [2]. A third scenario is that the orbit of a critical point enters T_λ at iteration 2 or higher. Then, by the above symmetry, all such critical orbits do the same. In this case, it is known that the Julia set is a Sierpiński curve [6], i.e., a set that is homeomorphic to the well known Sierpiński carpet fractal. The regions in the parameter plane for which this happens are the open disks that we call Sierpiński holes [13]. If the critical orbits do not escape to ∞, then it is known [8] that the Julia set is a connected set. Thus we call the set of parameters for which the critical orbits either do not escape or else enter the trap door at iteration 2 or higher the connectedness locus. This is the region between the Cantor set locus and the McMullen domain. In [1] it has been shown that there is a "principal" Mandelbrot set $\mathcal{M}^1$ in the parameter plane that lies along the positive real axis and extends from the Cantor set locus down to the McMullen domain. See Figure 4 for a display of these regions in the parameter plane. For more details about the dynamical properties of these maps and structure of the parameter plane, see [3].

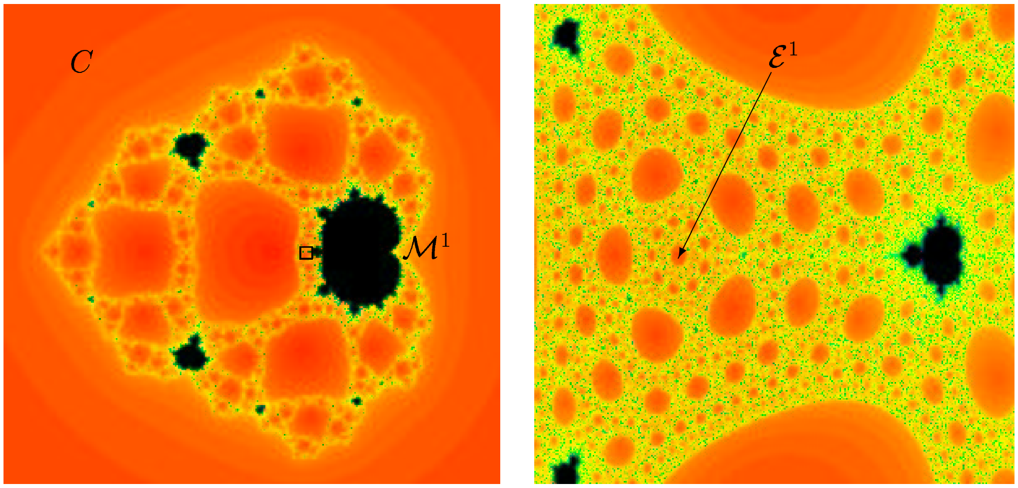

Figure 4: The parameter plane for the family $z^2+\lambda/z^3$. The external region C is the Cantor set locus. All of the disks visible in these pictures are Sierpiński holes, except for the McMullen domain M, which is the tiny disk pointed to in the magnification. The principal Mandelbrot set lies along the positive real axis between the Cantor set locus and the McMullen domain.

2 The Initial Mandelpinski Arc

In this section, we construct a Mandelpinski arc. This will be an arc in the parameter plane that passes alternately along the spines of infinitely many baby Mandelbrot sets and through the centers of the same number of Sierpiński holes. By the spine of the Mandelbrot set we mean the analogue of the portion of the real axis lying in the usual Mandelbrot set associated with the quadratic family $z^2 + c$. As a remark, the construction in this section replicates the one in [4], but we include these ideas here since they are essential for what comes later.

In this first case, there will be infinitely many Mandelbrot sets $\mathcal{M}^k$ with $k \geq 2$ along this arc. Here k is the period of the attracting cycle for parameters drawn from the main cardioid of $\mathcal{M}^k$, i.e., the base period of $\mathcal{M}^k$. There will also be infinitely many Sierpiński holes $\mathcal{E}^k$ with $k \geq 1$ where k is the escape time in $\mathcal{E}^k$, i.e., the number of iterations it takes for the orbit of the critical points to enter T_λ. In this special case, the arc will be the portion of the negative real axis in the parameter plane extending from the McMullen domain $\mathcal{E}^1$ down to the endpoint on the boundary of the connectedness locus. Then the Mandelbrot sets and Sierpiński holes will be arranged along this arc as follows:

$$\ldots \mathcal{M}^4 < \mathcal{E}^3 < \mathcal{M}^3 < \mathcal{E}^2 < \mathcal{M}^2 < \mathcal{E}^1.$$

In each case there will be an interval of nonzero length between any adjacent Mandelbrot set and Sierpiński hole lying along this arc. The Mandelpinski spokes we construct later will emanate from each of the $\mathcal{M}^k$.

To construct the objects lying along this arc, we will restrict attention at first to the λ-values lying in the annular region $\mathcal{O}$ in parameter plane given by $10^{-10} \leq |\lambda| \leq 2$. Also, let $\mathcal{A}$ be the annulus in the dynamical plane given by $\kappa 10^{-4} \leq |z| \leq \kappa 2^{2/5}$ where $\kappa \approx 1.96$ is defined as above.

Proposition.

1. *For any $\lambda \in \mathcal{O}$, all points on the outer circular boundary of $\mathcal{A}$ lie in B_λ, while all points on the inner circular boundary of $\mathcal{A}$ lie in T_λ. Moreover, F_λ maps each of these boundaries strictly outside the outer boundary of $\mathcal{A}$.*

2. *If λ lies on the inner circular boundary of $\mathcal{O}$, then each critical value lies on the inner circular boundary of $\mathcal{A}$ and so λ lies in the McMullen domain.*

3. *If λ lies on the outer circular boundary of $\mathcal{O}$, then each critical value lies on the outer circular boundary of $\mathcal{A}$ and so λ lies in the Cantor set locus in the parameter plane.*

Proof: First, if $|z| = \tau\kappa 2^{2/5}$ for any $\tau \geq 1$, we have for each $\lambda \in \mathcal{O}$:

$$\begin{aligned} |F_\lambda(z)| &\geq |\tau^2\kappa^2 2^{4/5}| - \left|\frac{\lambda}{\tau^3\kappa^3 2^{6/5}}\right| \\ &\geq \tau^2 1.95^2 2^{4/5} - \frac{2}{\tau^3\kappa^3 2^{6/5}} \\ &\geq 6\tau^2 - 1/(7\tau^3) \\ &> \tau\kappa 2^{2/5} = |z|. \end{aligned}$$

So all points outside of the circle $|z| = \kappa 2^{2/5}$ lie in B_λ when $\lambda \in \mathcal{O}$.

Similarly, if $|z| = \kappa 10^{-4}$, then we have

$$|F_\lambda(z)| \geq \frac{|\lambda|}{\kappa^3 10^{-12}} - \kappa^2 10^{-8} \geq \frac{10^{-10}}{\kappa^3 10^{-12}} - \kappa^2 10^{-8} \geq 100/\kappa^2 - \epsilon$$

where $\epsilon \approx 4 \cdot 10^{-8}$. So this inner boundary is mapped into B_λ and outside of $\mathcal{A}$, and so are all smaller circles around the origin. Hence this circle lies in T_λ (when λ lies in the connectedness locus).

Now if λ lies on the inner circular boundary of $\mathcal{O}$, then $|\lambda| = 10^{-10}$ so that $|v_j^\lambda| = \kappa 10^{-4}$ for each j. Hence, for these λ-values, v_j^λ lies on the inner circular boundary of $\mathcal{A}$, which lies in T_λ, and λ therefore lies in the McMullen domain. If λ lies on the outer circular boundary of $\mathcal{O}$, then $|\lambda| = 2$ so that $|v_j^\lambda| = \kappa 2^{2/5}$ (the outer boundary of $\mathcal{A}$) and thus this boundary circle lies in the Cantor set locus in the parameter plane.

$\square$

We now restrict attention to a "smaller" subset of $\mathcal{O}$. Let $\mathcal{O}'$ be the subset of $\mathcal{O}$ containing parameters λ for which $0 \leq \operatorname{Arg}\lambda \leq 2\pi$. Despite the overlap of this region along the real axis, we will think of $\mathcal{O}'$ as being a closed disk (not an annulus) in the parameter plane with $\operatorname{Arg}\lambda = 0$ and $\operatorname{Arg}\lambda = 2\pi$ considered as different portions of the boundary. We do this because, as $\operatorname{Arg}\lambda$ increases from 0 to 2π, the critical point c_0 that we will be following rotates one-fifth of a turn in the dynamical plane. So this point will migrate to the position of a different critical point as $\operatorname{Arg} \lambda$ rotates one full turn.

For any parameter in $\mathcal{O}'$, let L^λ be the closed "portion of the wedge" in the annulus $\mathcal{A}$ in the dynamical plane that is bounded by the two prepole rays through p_0 and p_{-1}. When $\lambda \in \mathbb{R}^-$, L^λ is thus bounded by the rays extending from 0 and passing through $\exp(2\pi i(2/5))$ and $\exp(2\pi i(3/5))$. So the critical point c_0 lies in the interior of L^λ. Next, let R^λ be the portion of the wedge in $\mathcal{A}$ that is bounded by the critical point rays passing through c_2 and c_{-2}. When $\lambda \in \mathbb{R}^-$, this wedge is bounded by the critical point rays extending from 0 and passing through $\exp(\pm 2\pi i/10)$. Note that R^λ is the symmetric image of L^λ under $z \mapsto -z$. See Figure 5.

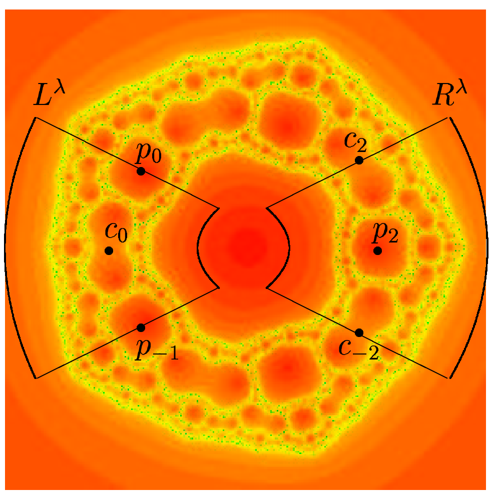

Figure 5: The wedges L^λ and R^λ for $\lambda = -0.09$.

Proposition. *For each* $\lambda \in \mathcal{O}'$*:*

1. F_λ *maps the interior of* R^λ *in one-to-one fashion onto a region that contains the interior of* $R^\lambda \cup L^\lambda$ *together with a portion of* T_λ *that*

contains 0*;*

2. F_λ *maps the interior of* L^λ *two-to-one over a region that contains the interior of* R^λ*;*

3. *As* λ *winds once around the boundary of* $\mathcal{O}'$*, the critical value* $F_\lambda(c_0^\lambda) = v_0^\lambda$ *winds once around the boundary of* R^λ*, (i.e., the winding index of the vector connecting this critical value to the prepole* p_2^λ *lying in the interior of* R^λ *is one).*

Proof: For the first case, recall that the straightline boundaries of R^λ are mapped two-to-one onto the critical value rays passing through v_2^λ and v_{-2}^λ. When $0 < \operatorname{Arg}\lambda < 2\pi$, one checks easily that these rays are disjoint from both R^λ and L^λ. The reason for this is that the arguments of the rays containing the critical values increase/decrease twice as fast as the arguments of the critical point and prepole rays as λ varies. However, when $\operatorname{Arg}\lambda = 0$, the critical value ray v_2^λ now reaches the boundary of R^λ on the real line, and when $\operatorname{Arg}\lambda = 2\pi$, the same thing is true for the critical value ray v_{-2}^λ. By the previous Proposition, the outer boundary curve of R^λ is mapped to an arc that lies in B_λ and also lies outside the outer circular boundaries of R^λ and L^λ. This image arc connects the two critical value rays in B_λ, and lies to the right of these rays in the basin. The inner boundary is mapped to a similar arc connecting these rays but now lying to the left of L^λ. Consequently, the image of R^λ contains the interiors of both R^λ and L^λ and a portion of T_λ, since the critical values never land at the origin. As a remark, R^λ is usually mapped one-to-one over T_λ; it is only when λ lies in the McMullen domain that this map is not one-to-one over T_λ because a critical value now lies in T_λ.

For the second case, we have that the straightline boundaries of L^λ contain the prepoles p_0^λ and p_{-1}^λ, which are both mapped to straight lines passing through the origin. In the case of p_0^λ, we have that p_0^λ lies on the straight line passing through the origin and $\exp(2\pi i(2/5))$ when $\lambda \in \mathbb{R}^-$. So the image of this straight line passes through $\exp(2\pi i(4/5))$ in this case. Then as $\operatorname{Arg}\lambda$ increases or decreases by at most π, the argument of this image line rotates by at most one-fifth of a turn in the corresponding direction. Hence this line lies strictly outside R^λ (except when $\operatorname{Arg}\lambda = 2\pi$, in which case this line is now the real axis, which meets the boundary of R^λ). Similar arguments work for the image of the other prepole ray. For the circular boundaries of L^λ, by the previous Proposition, they are both mapped to curves in B_λ that lie outside of the outer boundary of $\mathcal{A}$, but now these curves are arcs that connect the images of the prepole rays passing to the right of these lines. Hence F_λ maps L^λ over the interior of R^λ in two-to-one fashion.

For the third case, when $\operatorname{Arg}\lambda = 0$, the image of c_0^λ lies on the ray passing through $\exp(-2\pi i/5)$, and when $\operatorname{Arg}\lambda = 2\pi$, this critical value lies on the complex conjugate ray. So, for these parameters, the critical value lies on a line that includes the straight line boundary of R^λ. For the circular boundaries of $\mathcal{O}'$, the previous Proposition shows that the critical value now rotates around in a region outside the corresponding circular boundary of R^λ. Hence the critical value $F_\lambda(c_0^\lambda)$ winds with index one around R^λ as λ winds around the boundary of $\mathcal{O}'$.

□

Before constructing this Mandelpinski arc, we recall the concept of a polynomial-like map. Let G_μ be a family of holomorphic maps that depends analytically on the parameter μ lying in some open disk $\mathcal{D}$. Suppose each $G_\mu : U_\mu \to V_\mu$ where both U_μ and V_μ are open disks that also depend analytically on μ. G_μ is then said to be polynomial like of degree 2 if, for each μ:

- G_μ maps U_μ two-to-one onto V_μ and so there is a unique critical point in U_μ;

- V_μ contains U_μ;
- As μ winds once around the boundary of $\mathcal{D}$, the critical value winds once around U_μ in the region $V_\mu - U_\mu$.

As shown in [9], for such a family of polynomial-like maps, there is a homeomorphic copy of the Mandelbrot set in the disk $\mathcal{D}$. Moreover, for μ-values in this Mandelbrot set, $G_\mu \,|\, U_\mu$ is conjugate to the corresponding quadratic map given by this homeomorphism.

We can now prove

Theorem. *Along the negative real axis in the parameter plane, there exist infinitely many alternating Mandelbrot sets $\mathcal{M}^k$ and Sierpiński holes $\mathcal{E}^k$ with $k \geq 2$. Here k denotes the base period of $\mathcal{M}^k$ and the escape time of $\mathcal{E}^k$.*

Proof: We first consider the escape time case. By construction, for each $\lambda \in \mathcal{O}'$, there is a unique prepole p_2^λ in the interior of R^λ. Since F_λ maps R^λ one-to-one over itself, there is a unique preimage of this prepole, z_3^λ, in R^λ, so $F_\lambda^2(z_3^\lambda) = 0$. Continuing, for each $\lambda \in \mathcal{O}'$, there is a unique point z_k^λ in R^λ for which we have $F_\lambda(z_k^\lambda) = z_{k-1}^\lambda$ and so $F_\lambda^{k-1}(z_k^\lambda) = 0$. Now the points z_k^λ vary analytically with λ and are strictly contained in the interior of R^λ. So we may consider the function $H^k(\lambda)$ defined on $\mathcal{O}'$ by $H^k(\lambda) = v_0^\lambda - z_k^\lambda$ where $v_0^\lambda = F_\lambda(c_0^\lambda)$. When λ rotates once around the boundary of $\mathcal{O}'$, v_0^λ rotates once around the boundary of R^λ while z_k^λ remains in the interior of R^λ. Hence $H^k(\lambda)$ has winding number one along the boundary of $\mathcal{O}'$ and so there must be a unique zero in $\mathcal{O}'$ for each H^k. This is then the parameter that lies at the center of the escape time region $\mathcal{E}^k$. It is well known [13] that $\mathcal{E}^k$ is then an open disk in the parameter plane. Note that, as λ decreases along $\mathbb{R}^-$, both v_0^λ and z_k^λ increase along $\mathbb{R}^+$. It then follows that the portion of $\mathcal{E}^{k+1}$ in $\mathbb{R}^-$ lies to the left of $\mathcal{E}^k$ in the parameter plane.

To prove the existence of the Mandelbrot sets $\mathcal{M}^k$, recall that the orbit of the point z_k^λ under F_λ remains in R^λ before entering T_λ and landing at 0 at iteration $k-1$ (here $z_2^\lambda = p_2^\lambda$). For each $k \geq 2$, let E_λ^k be the open set surrounding z_k^λ in R^λ that is mapped onto T_λ by F_λ^{k-1}. Let D_λ^k be the set in R^λ consisting of points whose first $k-2$ iterations lie in R^λ but whose $(k-1)^{\text{st}}$ iterate lies in the interior of L^λ. Since F_λ is univalent on R^λ, each D_λ^k is an open disk. Furthermore, the boundary of D_λ^k meets a portion of the boundaries of both E_λ^{k-1} and E_λ^k (where $E_\lambda^1 = T_\lambda$). Since F_λ^{k-1} maps D_λ^k one-to-one over the interior of L^λ and then F_λ maps L^λ two-to-one over a region that contains R^λ, we have that F_λ^k maps D_λ^k two-to-one over a region that completely contains R^λ. Moreover, the critical value for F_λ^k is just v_0^λ, which, by the preceding Proposition, winds once around the exterior of R^λ as λ winds once around the boundary of $\mathcal{O}'$. Hence F_λ^k is a polynomial-like map of degree two on D_λ^k and this proves the existence of a baby Mandelbrot set $\mathcal{M}^k$ lying in $\mathcal{O}'$ for each $k \geq 2$. When λ is real and negative, we have that the centers of the escape regions $\mathcal{E}^k$ lie along $\mathbb{R}^-$ and, since the real line is invariant under F_λ when $\lambda \in \mathbb{R}^-$, both c_0^λ and v_0^λ also lie on the real axis. Then, by the $\lambda \mapsto \overline{\lambda}$ symmetry in the parameter plane, the spines of these Mandelbrot sets also lie in $\mathbb{R}^-$.

Next, since the E_λ^k and D_λ^k are arranged along the positive real axis in the following fashion:

$$T_\lambda = E_\lambda^1 < D_\lambda^2 < E_\lambda^2 < D_\lambda^3 < E_\lambda^3 < \dots$$

and, as shown above, the $\mathcal{E}^k$ decrease along $\mathbb{R}^-$ as k increases. Thus we have that the $\mathcal{E}^k$ and $\mathcal{M}^k$ are arranged along the negative real axis in the parameter plane in the opposite manner:

$$\dots \mathcal{E}^3 < \mathcal{M}^3 < \mathcal{E}^2 < \mathcal{M}^2 < \mathcal{E}^1.$$

See Figure 6.

Finally, when $\lambda \in \mathbb{R}^-$, there is a non-empty interval lying between each adjacent $\mathcal{M}^k$ and $\mathcal{E}^j$ (where $j = k$ or $k-1$). This interval contains parameters for which $F_\lambda^k(c_0^\lambda)$ lies in L^λ, but then $F_\lambda^{k+1}(c_0^\lambda)$ is back in R^λ and close to ∂B_λ. As a consequence, it takes more than k additional iterations for this critical orbit to reach T_λ or return to L^λ.

$\square$

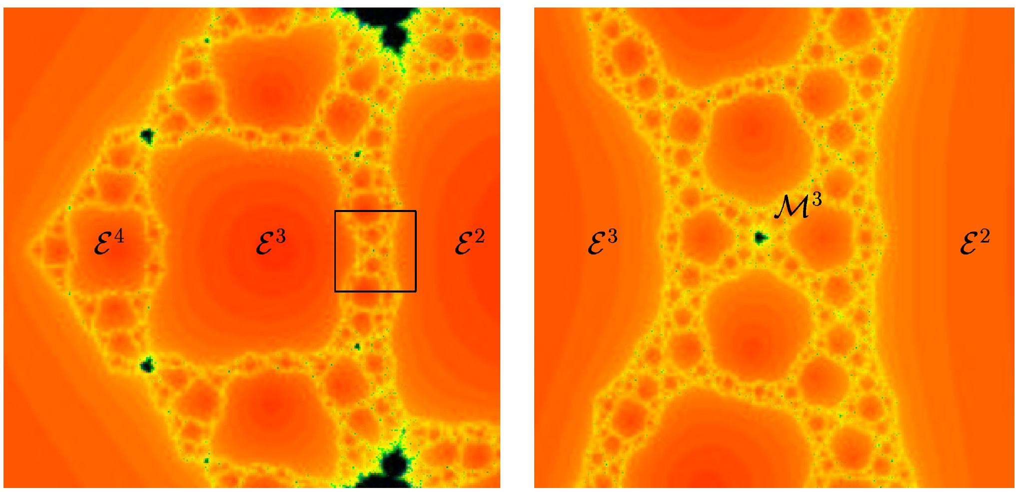

Figure 6: The Mandelpinski arc along the negative real axis. The $\mathcal{M}^k$ are so small that they are not visible in this picture. However, the magnification shows $\mathcal{M}^3$.

In the remainder of this paper, we shall concentrate on a specific Mandelbrot set $\mathcal{M}^k$ and describe the infinite collection of Mandelpinski spokes emanating from this set. With an eye toward how we shall proceed with this construction, note that, at this stage, we have a single infinite Mandelpinski arc extending to the left of $\mathcal{M}^k$ which contains the sets $\mathcal{M}^j$ with $j > k$ and $\mathcal{E}^j$ with $j \geq k$. And there is a finite Mandelpinski arc lying on the other side of $\mathcal{M}^k$ which now contains finitely many sets $\mathcal{M}^j$ where $2 \leq j < k$

and $\mathcal{E}^j$ where $1 \leq j < k$. These will be the initial portions of two of the Mandelpinski spokes emanating from $\mathcal{M}^k$.

3 The First Mandelpinski Spoke

In this next phase of the construction, we shall show that, on each side of the Mandelbrot set $\mathcal{M}^k$ in the first spoke, there are a pair of infinite spokes, each extending over to one of the adjacent Sierpiński holes $\mathcal{E}^k$ and $\mathcal{E}^{k-1}$. We think of this as extending the two previously constructed arcs emanating from $\mathcal{M}^k$. In addition, we shall show that there are a pair of new finite spokes extending above and below each $\mathcal{M}^k$. As above, a finite spoke means that there are only finitely many Mandelbrot sets and Sierpiński holes that alternate along this spoke. These will be the initial portions of the first four spokes emanating from $\mathcal{M}^k$.

To begin this phase of the construction, let us assume that the critical value v_0^λ now lies in a particular open disk D_λ^k for some fixed $k \geq 2$. Let $\mathcal{O}_k \subset \mathcal{O}'$ denote the set of parameters for which this happens. Now the boundary of D_λ^k is mapped by F_λ^{k-1} one-to-one onto the boundary of L^λ, and the boundary of L^λ varies analytically with λ. So we can construct a natural parametrization of this boundary which also varies analytically with λ. Then we can pull back this parameterization to the boundary of each D_λ^k. Again, as we saw earlier, as λ rotates around the boundary of the original disk $\mathcal{O}'$ in the parameter plane, v_0^λ rotates once around the boundary of R^λ. Hence, arguing just as in the previous section, there must be a unique parameter λ for which v_0^λ lands on any given point in the parametrization of the boundary of D_λ^k. Hence we have that $\mathcal{O}_k$ is a disk contained inside $\mathcal{O}'$ and, as λ rotates once around the boundary of $\mathcal{O}_k$, the critical value has winding number one around the boundary of the disk D_λ^k.

Now consider the set of preimages in L^λ of all of the D_λ^j and E_λ^j under F_λ. Since we have assumed that v_0^λ lies in D_λ^k, it follows that there is a unique preimage of D_λ^k in L^λ which is a disk that contains c_0^λ and is mapped two-to-one onto D_λ^k. Call this special disk L_k^λ. For each other D_λ^j (with $j \neq k$), there are now two preimage disks lying in L^λ. Note that, when $\lambda \in \mathbb{R}^-$ and $j > k$, there are a pair of preimages of D_λ^j lying along $\mathbb{R}^-$, one to the right of L_k^λ and one to the left. These preimages tend away from D_λ^k in either direction as j increases. When $2 \leq j < k$, there are again two preimages of D_λ^j, but when $\lambda \in \mathbb{R}^-$, these preimages no longer lie on the negative axis; rather they branch out more or less perpendicularly above and below L_k^λ on this axis. As for the preimages of E_λ^j in L^λ, we have the same situation: there are infinitely many pairs of preimages of each E_λ^j lying along $\mathbb{R}^-$ on either side of the preimage of D_λ^k when $j \geq k$ and $\lambda \in \mathbb{R}^-$, and finitely many pairs extending above and below this preimage when $1 \leq j < k$. Thus we have a pair of infinite chains of alternating preimages of the disks D_λ^k and E_λ^k extending away from L_k^λ and another pair of chains consisting of finitely many such preimages extending in a "perpendicular" direction away from L_λ^k.

Since F_λ^{k-1} maps D_λ^k one-to-one over L^λ, we thus have a similar collection of preimages that lie inside the disk D_λ^k. We denote by D_λ^{kj} each of the two disks in D_λ^k that are mapped onto D_λ^j by F_λ^k when $j \neq k$. And we let D_λ^{kk} denote the single preimage of D_λ^k under F_λ^k that is contained in D_λ^k, i.e., the preimage of L_k^λ under F_λ. So points in D_λ^{kj} have orbits that remain in R^λ for the first $k-2$ iterations, then map to L^λ under the next iteration, and then map into D_λ^j under the next iteration. Then F_λ^{j-1} maps this set onto L^λ. So F_λ^{k+j-1} maps each D_λ^{kj} one-to-one onto all of L^λ (assuming $k \neq j$). Then the next iteration takes this set two-to-one onto all of R^λ. Now the critical value for F_λ^{k+j} is again v_0^λ, and, as we showed above, as λ rotates around the boundary of $\mathcal{O}_k$, v_0^λ circles around the boundary of D_λ^k. Hence F_λ^{j+k} is polynomial-like of degree two on each of the two disks D_λ^{kj} (where we again emphasize that we are assuming $j \geq 2$ and $j \neq k$). So this produces a pair of Mandelbrot sets $\mathcal{M}^{kj}$ with base period $k+j$ in $\mathcal{O}_k$. As in the previous construction, the Mandelbrot sets $\mathcal{M}^{kj}$ with $j > k$ all have spines lying along $\mathbb{R}^-$, one on each side of $\mathcal{M}^k$. The other Mandelbrot sets with $j < k$ now lie off the real axis, one above $\mathcal{M}^k$ and the other below $\mathcal{M}^k$.

Similar arguments as in the preceding section also produce a pair of Sierpiński holes $\mathcal{E}^{kj}$ on each side of $\mathcal{M}^k$ along the real axis where now $j \geq k$. And there are a pair of Sierpiński holes $\mathcal{E}^{kj}$, one above and one below $\mathcal{M}^k$, where now $1 \leq j < k$. As earlier, these Mandelbrot sets and Sierpiński holes alternate along each of these spokes. For parameters in the Sierpiński hole $\mathcal{E}^{k1}$, the critical orbit $F_\lambda^i(c_0^\lambda)$ lies in R^λ for iterations $1 \leq i \leq k-1$. Then $F_\lambda^k(c_0^\lambda)$ returns to L^λ, and then $F_\lambda^{k+1}(c_0^\lambda)$ enters T_λ.

Note that the Mandelbrot sets $\mathcal{M}^{kj}$ are not subsets of the larger Mandelbrot set $\mathcal{M}^k$. This follows since the orbit of the critical point returns to L^λ only at iterations k and $k+j$ with $j \neq k$ when $\lambda \in \mathcal{M}^{kj}$, whereas these returns occur at iterations k and $2k$ when $\lambda \in \mathcal{M}^k$. This also follows from the fact that there is a Sierpiński hole separating each of these baby Mandelbrot sets from $\mathcal{M}^k$ along the new spoke. In Figure 7 we display a portion of these smaller spokes around $\mathcal{M}^4$. To summarize the results at this phase of the construction, we have shown:

Theorem. *In the original Mandelpinski arc, between each $\mathcal{E}^{k-1}$ and $\mathcal{E}^k$, there exist a pair of infinite spokes, each containing Mandelbrot sets $\mathcal{M}^{kj}$ where $j > k$ and Sierpiński holes $\mathcal{E}^{kj}$ where $j \geq k$ in the same alternating arrangement as earlier. One spoke extends from $\mathcal{M}^k$ to $\mathcal{E}^{k-1}$, the other from $\mathcal{M}^k$ to $\mathcal{E}^k$. The are also a pair of finite spokes extending away from $\mathcal{M}^k$ in different directions. These finite spokes contain the Mandelbrot sets $\mathcal{M}^{kj}$*

where $2 \leq j < k$ and the Sierpiński holes $\mathcal{E}^{kj}$ where now $1 \leq j < k$. The Mandelbrot sets $\mathcal{M}^{kj}$ have base period $k+j$ and the Sierpiński holes $\mathcal{E}^{kj}$ have escape time $k+j$.

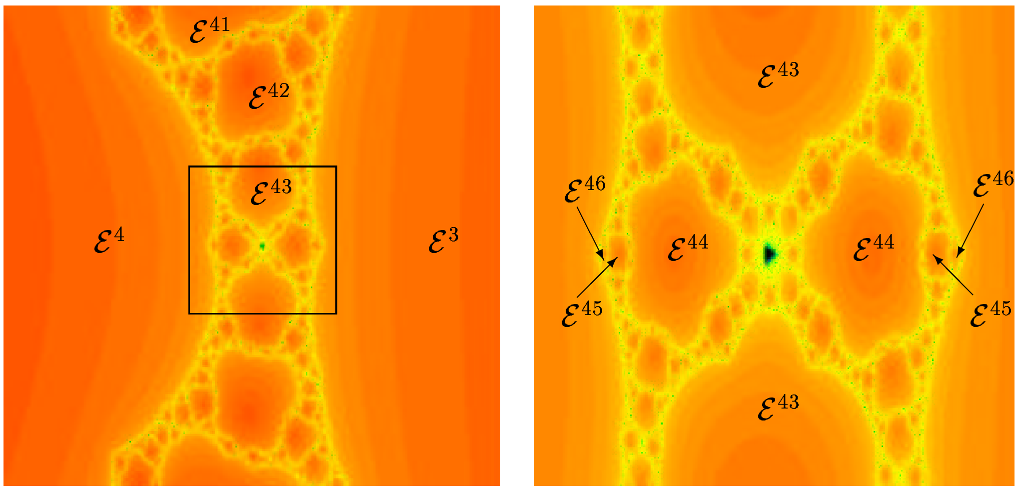

Figure 7: The finite spoke above and below $\mathcal{M}^4$ as well as a magnification showing the infinite spokes along the real axis.

4 Final Phase

We now continue the construction of the Mandelpinski spokes by induction. For simplicity, we will only consider the next phase of the construction; all subsequent phases follow in exactly the same way. This time we will adjoin four infinite spokes that lie closer to $\mathcal{M}^k$ to those already in place, and then we will add four new finite spokes in betwen each of these infinite spokes.

To be precise, in the previous phase, we assumed that the critical value resided in a particular disk D_λ^k, and so there was a special disk $D_\lambda^{kk} \subset D_\lambda^k$ that was mapped two-to-one onto D_λ^k by F_λ^k. At this stage we make the further assumption that v_0^λ lies in D_λ^{kk}. Let $\mathcal{O}_{kk} \subset \mathcal{O}_k$ be the set of parameters for which this occurs. Note that $\mathcal{M}^k$ lies in $\mathcal{O}_{kk}$. We have that F_λ^k maps the boundary of D_λ^{kk} two-to-one onto the boundary of D_λ^k. Thus we may pull back the parametrization of ∂D_λ^k constructed earlier to produce a natural parametrization of ∂D_λ^{kk} which varies analytically with λ. Thus there is a unique λ for which v_0^λ lands on a given point in the boundary of D_λ^{kk}, and so, as λ winds once around the boundary of $\mathcal{O}_{kk}$, v_0^λ winds once around ∂D_λ^{kk}.

By the prior construction, we have a pair of infinite chains each of which consists of the disks D_λ^{kj} with $j > k$ and E_λ^{kj} with $j \geq k$ lying in the annular region $D_\lambda^k - D_\lambda^{kk}$ as well as a pair of finite chains consisting of the disks D_λ^{kj} and E_λ^{kj} with $j < k$ lying in the same annulus. Since F_λ^k maps D_λ^{kk} two-to-one onto the entire disk D_λ^k, we therefore have four new infinite chains inside D_λ^{kk} that are the preimages of the two infinite chains in the annular region. These chains consist of disks that we denote by either D_λ^{kkj} with $j > k$ or E_λ^{kkj} with $j \geq k$. Each of these chains then connects to one of the two infinite or finite chains in the outer annular region. This follows since these outer chains were all mapped onto the left or right portion of the original chain by F_λ^k. We also have four finite chains in D_λ^{kk} consisting of disks D_λ^{kkj} and E_λ^{kkj} with $j < k$ that are preimages of the finite chains in the annular region. These chains do not connect to the previously constructed chains in the annular region.

Then the same arguments as above produce the corresponding spokes in the parameter plane. Each of the two finite and infinite spokes constructed earlier now have an added infinite spoke that lies in the region between $\mathcal{M}^k$ and that spoke. The Mandelbrot sets and Sierpiński holes in this new portion of the spoke are given by $\mathcal{M}^{kkj}$ where $j > k$ and $\mathcal{E}^{kkj}$ where $j \geq k$ and the four new finite spokes consist of similar sets with now $j < k$. These are all associated with rays of angle $\ell/8$ with ℓ even for the infinite spokes and ℓ odd for the finite spokes.

At this stage we now have eight Mandelpinski spokes emanating from $\mathcal{M}^k$, four finite spokes and four infinite spokes. Continuing inductively, at the next stage, we then add eight infinite spokes between each of these spokes and $\mathcal{M}^k$ as well as eight new finite spokes, one between each of these newly added infinite spokes. In the limit, we get an infinite collection of Mandelpinski spokes emanating from $\mathcal{M}^k$.

References

[1] Devaney, R. L. Baby Mandelbrot Sets Adorned with Halos in Families of Rational Maps. In *Complex Dynamics; Twenty-Five Years After the Appearance of the Mandelbrot Set.* Amer. Math. Soc. Contemporary Math. **396** (2006), 37-50.

[2] Devaney, R. L. Structure of the McMullen Domain in the Parameter Planes for Rational Maps. *Fund. Math.* **185** (2005), 267-285.

[3] Devaney, R. L. Singular Perturbations of Complex Polynomials. *Bulletin of the AMS* **50** (2013), 391-429.

[4] Devaney, R. L. A Mandelpinski Maze for Rational Maps of the Form $z^n + \lambda/z^d$. To appear.

[5] Devaney, R. L. Cantor Necklaces and Structureally Unstable Sierpiński Curve Julia Sets for Rational Maps. *Qual. Thy. Dyn. Sys.* **5** (2004), 337-359.

[6] Devaney, R. L. and Look, D. M. A Criterion for Sierpiński Curve Julia Sets. *Topology Proceedings* **30** (2006), 163-179.

[7] Devaney, R. L., Look, D. M., and Uminsky, D. The Escape Trichotomy for Singularly Perturbed Rational Maps. *Ind. Univ. Math. J.* **54** (2005), 1621-1634.

[8] Devaney, R. L. and Russell, E. D. Connectivity of Julia Sets of Singularly Perturbed Rational Maps. In *Chaos, CNN, Memristors and Beyond*. World Scientific Press (2013), 239-245.

[9] Douady, A. and Hubbard, J. On the Dynamics of Polynomial-like Mappings. *Ann. Sci. ENS Paris* **18** (1985), 287-343.

[10] McMullen, C. Automorphisms of Rational Maps. *Holomorphic Functions and Moduli*. Vol. 1. Math. Sci. Res. Inst. Publ. **10** Springer, New York, 1988.

[11] Milnor, J. *Dynamics in One Complex Variable.* Princeton University Press, 2006.

[12] Moreno Rocha, M. A Combinatorial Invariant for Escape Time Sierpiński Rational Maps. *Funda. Math.* **222** (2013), 99-130.

[13] Roesch, P. On Captures for the Family $f_\lambda(z) = z^2 + \lambda/z^2$. In *Dynamics on the Riemann Sphere*. European Mathematical Society (2006), 121-130.